JACS
JOURNAL OF THE AMERICAN CHEMICAL SOCIETY
Article
pubs.acs.org/JACS

A New Type of Strong Metal–Support Interaction and the Production of H_2 through the Transformation of Water on Pt/CeO_2(111) and Pt/CeO_x/TiO_2(110) Catalysts

Albert Bruix,[†] José A. Rodriguez,*[,‡] Pedro J. Ramírez,[§] Sanjaya D. Senanayake,[‡] Jaime Evans,[§] Joon B. Park,[‡] Dario Stacchiola,[‡] Ping Liu,[‡] Jan Hrbek,[‡] and Francesc Illas[†]

[†]Departament de Química Física and Institut de Química Teòrica i Computacional (IQTCUB), Universitat de Barcelona, Marti i Franques 1, 08028 Barcelona, Spain

[‡]Chemistry Department, Brookhaven National Laboratory, Upton, New York 11973, United States

[§]Facultad de Ciencias, Universidad Central de Venezuela, Caracas 1020-A, Venezuela

ABSTRACT: The electronic properties of Pt nanoparticles deposited on CeO_2(111) and CeO_x/TiO_2(110) model catalysts have been examined using valence photoemission experiments and density functional theory (DFT) calculations. The valence photoemission and DFT results point to a new type of "strong metal–support interaction" that produces large electronic perturbations for small Pt particles in contact with ceria and significantly enhances the ability of the admetal to dissociate the O–H bonds in water. When going from Pt(111) to Pt_8/CeO_2(111), the dissociation of water becomes a very exothermic process. The ceria-supported Pt_8 appears as a fluxional system that can change geometry and charge distribution to accommodate adsorbates better. In comparison with other water-gas shift (WGS) catalysts [Cu(111), Pt(111), Cu/CeO_2(111), and Au/CeO_2(111)], the Pt/CeO_2(111) surface has the unique property that the admetal is able to dissociate water in an efficient way. Furthermore, for the codeposition of Pt and CeO_x nanoparticles on TiO_2(110), we have found a transfer of O from the ceria to Pt that opens new paths for the WGS process and makes the mixed-metal oxide an extremely active catalyst for the production of hydrogen.

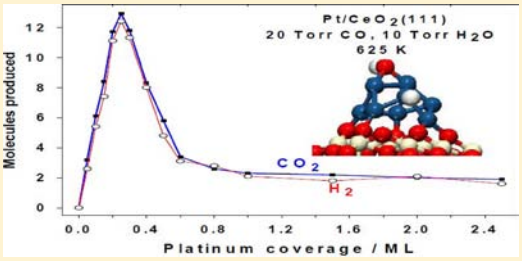

INTRODUCTION

Metal–oxide interfaces play a key role in a large set of technologically important applications such as metal–oxide contacts in microelectronics and photovoltaic devices, gas sensors, coatings for electrochemical devices or corrosion passivation, and oxide-supported transition-metal catalysts.[1] Over the years, a large number of studies have been focused on improving our understanding of the atomic-level structure of metal–oxide interfaces, the electronic character of the metal atoms that are right at these interfaces, and the energetics of bonding and thermodynamic stability of these interfaces.[1,2] These are critical issues connected to technological applications. In a classic article, Tauster et al.[3a] used the term "strong metal–support interaction" to describe the drastic changes that occur in the chemisorption properties of Pt and other group VIII (8–10) metals when they are dispersed on surfaces of titanium oxide. The ability to chemisorb H_2 or CO was strongly suppressed or vanished entirely when these metals were supported on TiO_2 and activated in H_2 at elevated temperatures.[3] A strong metal–support interaction had somehow deprived these metals of one of their most characteristic chemical properties, making them catalytically inactive.[3] The spreading of TiO_x aggregates on the surface of the supported metals could be responsible for the reduction in their chemical and catalytic activity.[3b,4] In this article, we report a completely different type of strong metal–support interaction that *substantially enhances* the catalytic activity of Pt for the generation of hydrogen through the water-gas shift (WGS) reaction, $CO + H_2O \rightarrow H_2 + CO_2$.

In industry, the WGS reaction is widely used to produce the hydrogen necessary for many chemical processes[5] and to eliminate the CO present in feed streams for ammonia synthesis and fuel cells.[6] There is a continuous search for new and more efficient WGS catalysts.[6,7] Supported platinum catalysts have received much interest during the past decade because of their WGS activity at low temperatures.[6−14] The WGS has been investigated over Pt nanoparticles (NPs) dispersed over various oxide supports: Al_2O_3, CeO_2, ZrO_2, CeO_2/ZrO_2, and TiO_2.[7−14] Among the oxide supports, the CeO_2 and TiO_2 substrates are two of the most promising candidates for the WGS process. The reason that the nature of the oxide is important for the good performance of Pt-based catalysts is a matter of debate.[6−14] Furthermore, a recent study of the WGS on Pt(111) indicates that there can be problems in performing the reaction on extended surfaces of platinum.[15] The turnover frequency of Pt(111) is initially 5 times greater than that observed on Cu(111), a typical benchmark for the

Received: March 1, 2012
Published: May 7, 2012

   dx.doi.org/10.1021/ja302070k | J. Am. Chem. Soc. 2012, 134, 8968–8974

WGS reaction,[16−18] but Pt(111) undergoes deactivation due to the deposition of carbon by the Boudouard reaction: $2CO(surf) \rightarrow C(surf) + CO_2(g)$.[15] Thus, why is Pt/CeO_2 a very good catalyst for the WGS reaction? In this work, we used experiment and theory to investigate the WGS reaction on well-defined $Pt/CeO_2(111)$ surfaces and to explain the high performance of the admetal in Pt/CeO_2 catalysts. The results of valence photoemission experiments and density functional theory (DFT) calculations point to a new type of strong metal−support interaction that produces large electronic perturbations for small Pt particles in contact with $CeO_2(111)$ and *significantly enhances* the ability of the admetal to dissociate the O−H bonds in water. Upon going from Pt(111) to $Pt_8/CeO_2(111)$, the dissociation of water becomes a very exothermic process. Furthermore, for the codeposition of Pt and CeO_x NPs on $TiO_2(110)$, we have found a transfer of O from the ceria to Pt that opens new paths for the WGS process and makes the mixed-metal oxide an extremely active catalyst for the production of hydrogen.

EXPERIMENTAL AND THEORETICAL METHODS

The photoemission and catalytic studies were carried out in a system combining an ultrahigh-vacuum (UHV) chamber (base pressure ~5×10^{-10} Torr) and a batch reactor.[18−20] The sample could be transferred between the reactor and the UHV chamber without exposure to air. The UHV chamber (base pressure ~5×10^{-10} Torr) was equipped with instrumentation for X-ray and UV photoelectron spectroscopies (XPS and UPS), low-energy electron diffraction (LEED), ion scattering spectroscopy (ISS), and temperature-programmed desorption (TPD). The microscopy studies were carried out in an Omicron variable-temperature scanning tunneling microscopy (STM) system directly attached to a main UHV chamber equipped with optics for LEED, instrumentation for Auger electron spectroscopy, and surface cleaning facilities. The kinetic tests were done using $CeO_2(111)$ and $TiO_2(110)$ single crystals cleaned following standard procedures used in our previous studies of $Au/CeO_2(111)$ and $Au/TiO_2(110)$.[19,20] To avoid problems with charging in the XPS and UPS experiments, films of $CeO_2(111)$ were grown in situ onto a Ru(0001) substrate (700 K) using a four-pocket Oxford evaporator in an O_2 atmosphere (1×10^{-7} Torr). Previous studies have been devoted to understanding this growth and the formation of well-defined (111) surfaces.[21,22] The Oxford evaporator was also used to deposit CeO_x on $TiO_2(110)$.[20,23] Pt was evaporated onto $CeO_2(111)$ and $CeO_x/TiO_2(110)$ at 300 K. In the kinetic measurements, the sample was transferred to the batch reactor at ~300 K, after which the reactant gases were introduced (20 Torr CO and 10 Torr H_2O) and the sample was rapidly heated to the reaction temperature of 625 K. The number of molecules produced was normalized to the active area exposed by the sample.[19,20] In our reactor, a steady-state regime for the production of H_2 and CO_2 was reached after 2−3 min of reaction time.

The DFT calculations were performed using the VASP program (version 4.6)[24] and the methodology described in refs 25 and 26. We used the PW91 exchange−correlation functional, and the description of stoichiometric and reduced ceria was achieved within the so-called GGA+U approach with a U value of 4 eV.[27,28] The kinetic energy cutoff was 415 eV.[24] The $Pt_8/CeO_2(111)$ calculations employed a slab of three CeO_2 (nine atomic) layers and a 3×4 surface cell. The space between neighboring slab images was 1.5 nm.[24] Complete geometry optimizations were carried out for NP models, and only atoms in the bottom O−Ce−O layer were kept fixed at the bulk positions during the local-minimum search in the slab calculations.

RESULTS AND DISCUSSION

We start by examining the catalytic properties of Pt on $CeO_2(111)$. Since Pt/CeO_2 powder catalysts typically have small loadings of the noble metal (<2 wt %),[6] we are particularly interested in low coverages of Pt on $CeO_2(111)$. STM has been used to study the growth mode of Pt on $CeO_2(111)$ films supported on Ru(0001).[29] Deposition of 0.2 monolayer (ML) of Pt on $CeO_2(111)$ at 300 K produces small metal NPs on the ceria terraces with a height of two atomic layers. The introduction of oxygen vacancies in the oxide surface to give $CeO_{1.88}(111)$ leads to a better dispersion of the Pt, and the small metal aggregates now exhibit a height of one or two atomic layers.[29] Using XPS and He-II UPS, we investigated the interaction of Pt with the $CeO_2(111)$ crystal. After depositing 0.1−0.2 ML of Pt on $CeO_2(111)$, we measured Pt $4f_{7/2}$ core-level binding energies that were 0.7−0.9 eV higher than that found for bulk metallic Pt (71.2 eV). At the same time, UPS spectra for the valence region of the $Pt/CeO_2(111)$ systems (Figure 1) exhibited a density of Pt 5d

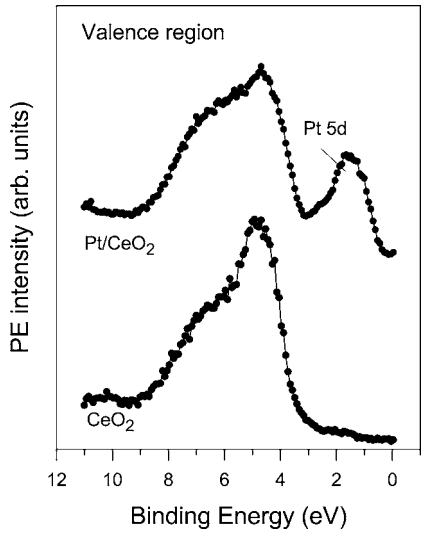

Figure 1. He-II valence UPS spectra collected before and after deposition of 0.15 ML of Pt on a $CeO_2(111)$ surface.

states near the Fermi level that was much smaller than that expected for metallic Pt.[30] In the case of Pt(111), a strong photoemission signal was observed between 0 and 1 eV,[30] whereas for $Pt/CeO_2(111)$ ($\theta_{Pt} < 0.25$ ML), there was a weak signal in this region. Small metal particles can exhibit a reduced density of d states near the Fermi edge when deposited on oxides.[1] Our results of photoelectron spectroscopy are consistent with previous experimental and theoretical studies that point to a Pt → ceria charge transfer when small particles of Pt are in contact with $CeO_2(111)$.[25,26] As we will show below, the perturbations in the electronic properties of the supported Pt NPs lead to an important change in their chemical properties.

Figure 2 displays the WGS activities of a large series of model $Pt/CeO_2(111)$ catalysts. The clean $CeO_2(111)$ surface did not have activity for the WGS reaction under the reaction conditions investigated here. Upon addition of Pt to $CeO_2(111)$, there was a continuous increase in the catalytic activity until a maximum was reached at a coverage of ~0.2 ML. After this point, the production of H_2 and CO_2 decreased drastically as the Pt coverage was raised. Postreaction surface characterization with XPS indicated that during the WGS process the ceria support was partially reduced, reaching a composition of $CeO_{1.90-1.93}$. Comparing these data with the STM results reported for the $Pt/CeO_2(111)$ and Pt/

dx.doi.org/10.1021/ja302070k | J. Am. Chem. Soc. 2012, 134, 8968−8974

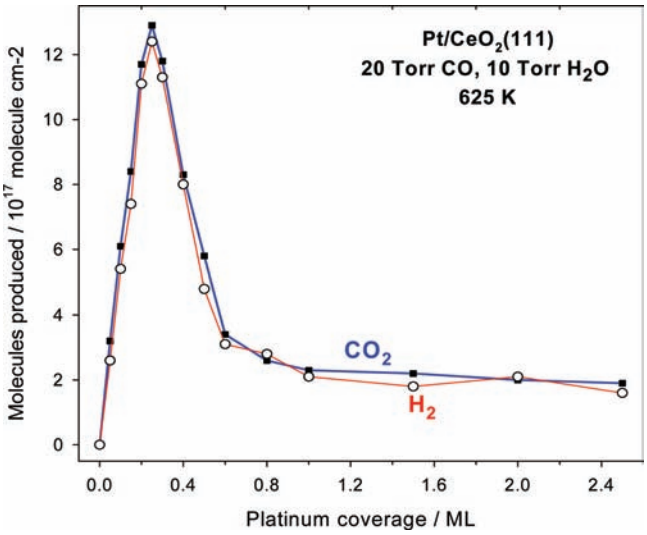

Figure 2. WGS activities of model $Pt/CeO_2(111)$ catalysts as a function of admetal coverage. Each surface was exposed to a mixture of 20 Torr CO and 10 Torr H_2O at 625 K for 5 min.

$CeO_{1.88}(111)$ systems,[29] one can conclude that the maximum activity in Figure 2 corresponds to catalysts that contain Pt particles with a diameter smaller than 1.7 nm and a height less than 0.4 nm. Furthermore, the measured catalytic activity is correlated with the magnitude of the electronic perturbations seen in UPS. The $Pt/CeO_2(111)$ catalysts with the highest activity (θ_{Pt} < 0.3 ML) displayed a lower density of Pt 5d states near the Fermi level (Figure 1), while the catalysts with lower activity (θ_{Pt} > 0.8 ML) exhibited a density of Pt 5d states near the Fermi level that was not much different from that of bulk metallic Pt(111).[30]

In test experiments, we found no signs of deactivation of the $Pt/CeO_2(111)$ (θ_{Pt} < 0.3 ML) catalysts after 2 h of reaction time. In the case of the WGS reaction on Pt(111), deactivation by deposition of carbon is observed after reaction times of 10–20 min.[15] Using plots for H_2 production versus time (Figure 3), we calculated the corresponding reaction rates and turnover numbers for the WGS reaction on $Pt/CeO_2(111)$. Assuming

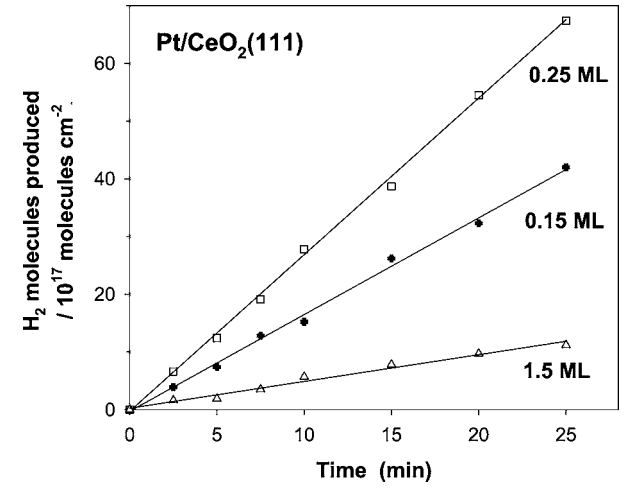

Figure 3. Numbers of H_2 molecules produced via the WGS reaction as functions of time on $Pt/CeO_2(111)$ catalysts containing 0.15, 0.25, and 1.5 ML of Pt. Each surface was exposed to a mixture of 20 Torr CO and 10 Torr H_2O at 625 K.

that all of the Pt atoms deposited on $CeO_2(111)$ participated in the reaction, we estimated turnover frequencies of 12.4 (θ_{Pt} = 0.15 ML) and 11.5 (θ_{Pt} = 0.25 ML) molecules Pt_{site}^{-1} s^{-1} for the highly active catalysts in Figure 2. These are *much larger* than the value of 0.53 molecules Pt_{site}^{-1} s^{-1} reported for Pt(111).[15] A comparison of the performance of $Pt/CeO_2(111)$ with those of catalysts containing Ni,[31] Cu,[20] or Au[20] dispersed on $CeO_2(111)$ (Figure 4) indicates that the Pt-based system is

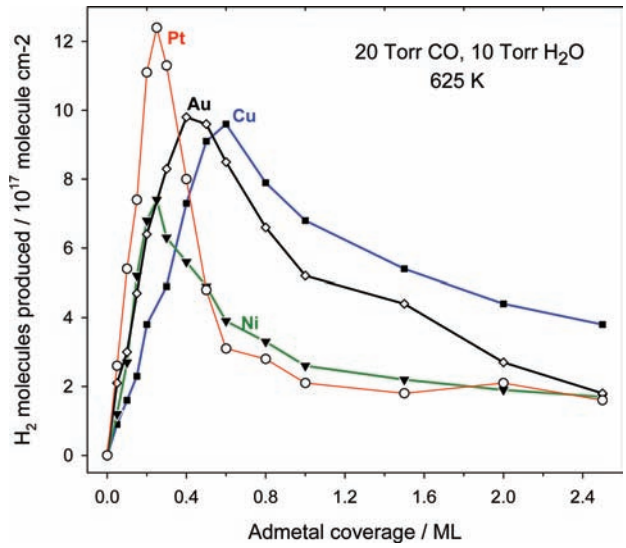

Figure 4. Numbers of H_2 molecules produced via the WGS reaction on catalysts generated by deposition of Pt (this work), Ni (ref 31), Cu (ref 20), and Au (ref 20), on $CeO_2(111)$. Each surface was exposed to a mixture of 20 Torr CO and 10 Torr H_2O at 625 K for 5 min.

clearly the best in terms of activity and low loading of the admetal under the conditions investigated in these studies (20 Torr CO and 10 Torr H_2O at 625 K). Systems such as $Au/CeO_2(111)$ and $Cu/CeO_2(111)$ exhibit better performance than $Pt/CeO_2(111)$ only at large loadings of the admetal (>0.3 ML), where the Pt catalytic activity substantially decreases, probably as a result of the fact that most of the Pt atoms are not in contact with the ceria support. A look at data reported in the literature for the performance of high-surface-area catalysts during the WGS reaction under various conditions also indicated that Pt/CeO_2 shows excellent activity.[6]

To enhance the interactions between Pt and ceria, we coadsorbed NPs of both on a $TiO_2(110)$ substrate. The properties of the $CeO_x/TiO_2(110)$ mixed metal oxide have been examined using STM and core and valence photoemission.[19,23] At small coverages, ceria deposited on $TiO_2(110)$ forms short wirelike nanostructures that contain dimers of Ce_2O_3 and exhibit a characteristic height of 1.4 ± 0.2 Å in STM.[19] On the other hand, the deposition of small coverages of Pt on clean $TiO_2(110)$ produces round particles with heights of 3–6 Å,[32] which is considerably larger than the height of the Ce_2O_3 dimers in $CeO_x/TiO_2(110)$.[19] From an analysis of the shape and height of the features in the STM image of $Pt/CeO_x/TiO_2(110)$ (Figure 5), one can identify three types of structures. The surface contains NPs of CeO_x with a wirelike structure and a height close to 1.4 Å (labeled as "a"). On top of or near the ceria structures, there are bright features with heights of 4–9 Å that correspond to Pt particles in direct contact with ceria (labeled as "b"). Finally, there are small round features that have heights of 3–5 Å that were not seen in

dx.doi.org/10.1021/ja302070k | J. Am. Chem. Soc. 2012, 134, 8968–8974

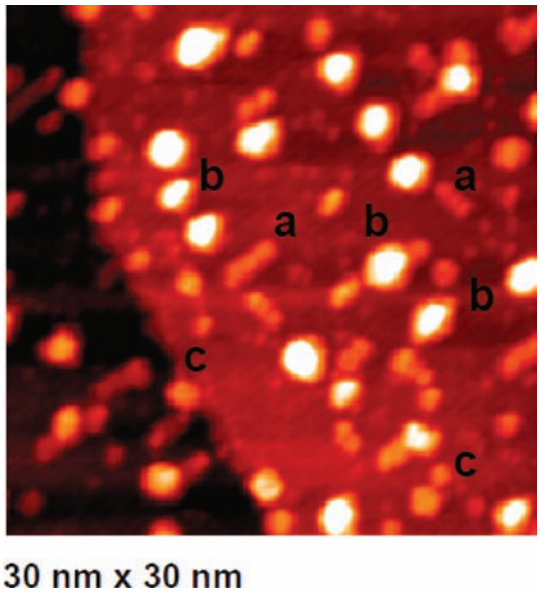

Figure 5. STM image taken after deposition of ~0.15 ML of Pt on a $CeO_x/TiO_2(110)$ surface. The deposition of Pt was done at 300 K, with subsequent heating to 625 K. The surface contains NPs of CeO_x with a wire-like structure (a), Pt particles on top of ceria (b, bright dots), and Pt particles on top of TiO_2 (c). Conditions: V_t = 1.2 V; I_t = 0.05 nA.

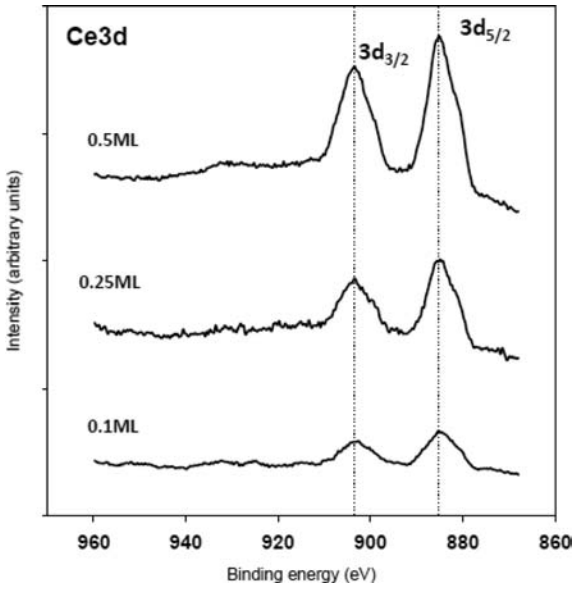

Figure 6. Ce 3d XPS spectra collected after deposition of 0.1, 0.25, or 0.5 ML of ceria on $TiO_2(110)$. Similar line shapes were found after the deposition of Pt.

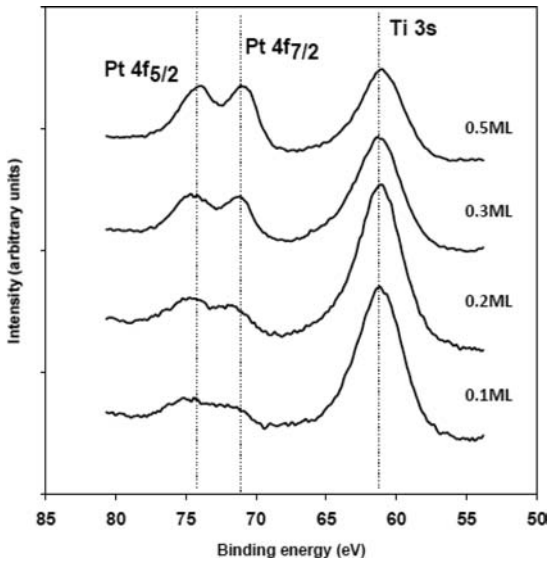

Figure 7. Pt 4f photoemission spectra collected after deposition of different coverages of Pt (0.1, 0.2, 0.3, or 0.5 ML) on a titania surface precovered with 0.2 ML of ceria. The unusual ratio of the intensities of the $^5/_2$ and $^7/_2$ peaks in the Pt 4f region points to the presence of some O on top of the Pt.[34]

STM images of $CeO_x/TiO_2(110)$[19] and probably correspond to Pt particles on top of the $TiO_2(110)$ substrate (labeled as "c").[32] When the CeO_x coverage on $TiO_2(110)$ was raised, STM showed the coalescence of the wirelike ceria nanostructures and the formation of three-dimensional islands.[23] In general, our STM results indicate that these ceria islands can act as excellent nucleation centers for the growth of Pt particles. Thus, in $Pt/CeO_x/TiO_2(110)$, there is close contact between Pt and ceria.

Ce 3d XPS data indicated Ce to be mainly in the +3 oxidation state in the $CeO_x/TiO_2(110)$ and $Pt/CeO_x/TiO_2(110)$ systems. Figure 6 shows Ce 3d XPS spectra collected after deposition of 0.1, 0.25, or 0.5 ML of ceria on $TiO_2(110)$. Similar line shapes were found after the deposition of Pt on the generated $CeO_x/TiO_2(110)$ surfaces. The line shapes shown in Figure 6 point to Ce^{3+} as the dominant cation species in the supported ceria.[33] The Ce 3d line shape for Ce^{4+} in stoichiometric CeO_2 is quite different.[33] UPS spectra taken after deposition of small amounts of Pt (0.1−0.2 ML) on $CeO_x/TiO_2(110)$ again showed a weak density of Pt 5d states near the Fermi level, as seen in the case of $Pt/CeO_2(111)$, indicating the existence of electronic perturbations in the admetal. The Pt 4f XPS spectra of $Pt/CeO_x/TiO_2(110)$ (Figure 7) exhibited a line shape with an apparent inversion of the usual ratio of intensities expected for the $^5/_2$ and $^7/_2$ peaks of metallic platinum.[34] This phenomenon has been seen before for the interaction of oxygen with platinum surfaces and is consistent with the presence of some O on the supported Pt NPs.[34] This is in agreement with recent results for Pt on nanostructured ceria showing a migration of O from the ceria to Pt that is not seen in the case of Pt deposited on a bulk $CeO_2(111)$ surface.[26]

Figure 8 shows the WGS activity of $Pt/TiO_2(110)$ and two sets of $Pt/CeO_x/TiO_2(110)$ catalysts in which 11 or 23% of the titania substrate was covered by ceria particles. The fraction of the titania covered by ceria was measured using ISS[19] before deposition of the Pt. The maximum activities were seen for catalysts containing a small amount of Pt (θ_{Pt} < 0.3 ML) and ceria (11% of the titania covered). These systems did not show signs of deactivation with time after kinetic tests of up to 2 h. The estimated turnover frequencies for catalysts containing 0.15 ML of Pt were 34.8 (11% of titania covered by ceria) and 28.6 (23% of titania covered by ceria) molecules Pt_{site}^{-1} s^{-1}. For this small Pt coverage, the $Pt/CeO_x/TiO_2(110)$ catalysts were 2.3−2.8 times more active than the corresponding $Pt/CeO_2(111)$ catalyst. On the other hand, at large coverages of Pt (>0.8 ML), when most of the metal adatoms are not affected by interactions with ceria and the Pt exhibits a large density of 5d states near the Fermi level, the catalytic activities of the Pt/

dx.doi.org/10.1021/ja302070k | J. Am. Chem. Soc. 2012, 134, 8968−8974

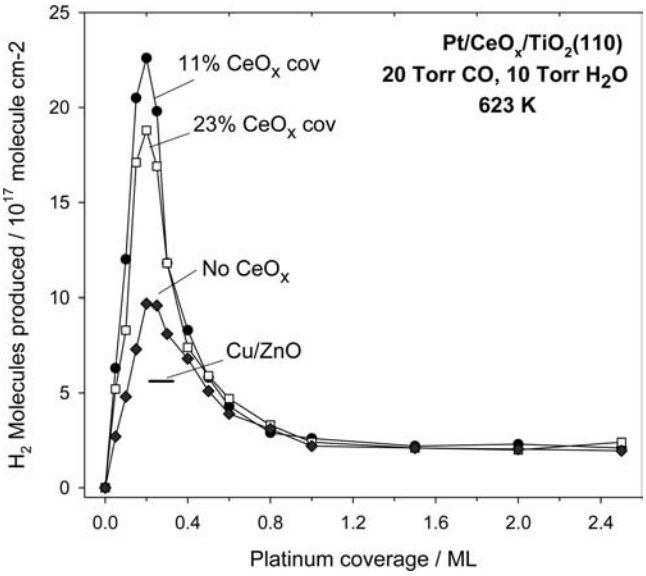

Figure 8. WGS activities of model Pt/TiO_2(110) and Pt/CeO_x/TiO_2(110) catalysts as functions of admetal coverage. Before vapor deposition of the Pt, ceria was dispersed on TiO_2(110) covering 11 and 23% of this substrate. Each surface was exposed to a mixture of 20 Torr CO and 10 Torr H_2O at 625 K for 5 min. For comparison, we have included the maximum activity found for the WGS reaction on the Cu/ZnO(000$\bar{1}$) system (θ_{Cu} = 0.5 ML).[20]

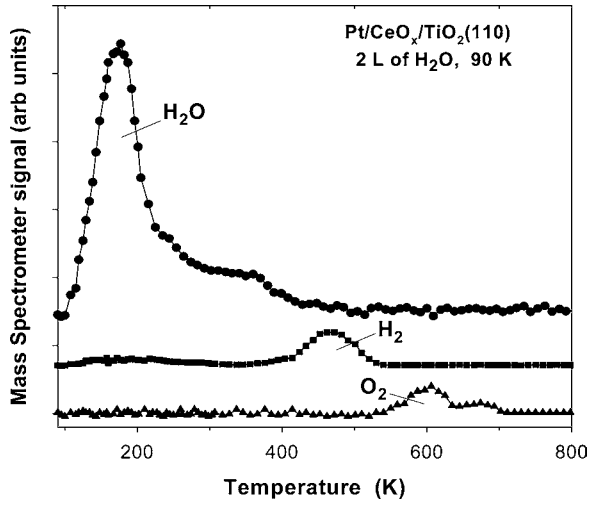

Figure 9. TPD spectra collected after dosing 2 langmuir of water onto a Pt/CeO_x/TiO_2(110) surface at ~90 K. The surface contained 0.2 ML of Pt, and ~11% of the titania was covered by ceria NPs.

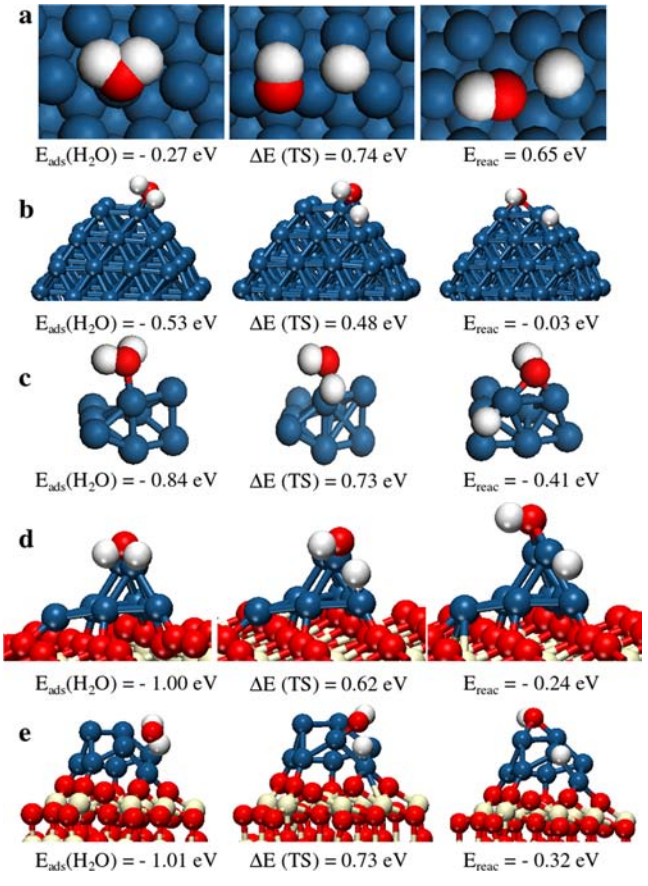

Figure 10. DFT-calculated structures for (left) adsorbed H_2O, (center) the transition state (TS), and (right) adsorbed HO + H along with the corresponding energy parameters [E_{ads}, ΔE(TS), E_{reac}] for the dissociation of water over (a) a Pt(111) surface, (b) a free Pt_{79} cluster, (c) a free Pt_8 cluster, and (d, e) Pt_8 clusters deposited on (d) a CeO_2(111) surface and (e) a $Ce_{40}O_{80}$ NP with a compact structure.[26] Pt, O, Ce, and H atoms are represented as blue, red, cream, and white spheres, respectively.

CeO_x/TiO_2(110) and Pt/CeO_2(111) systems are very close and similar to that of bulk Pt.

Cu/ZnO catalysts are frequently used in industrial processes for the production of hydrogen via the WGS reaction.[5,6] Pt/CeO_x/TiO_2 exhibits a WGS activity substantially higher than those of Cu/ZnO(000$\bar{1}$)[20] and Pt/TiO_2, Pt/CeO_2, and clean Pt(111).[15] Pt gets activated by electronic interactions with ceria, and these Pt ↔ CeO_x interactions seem to be stronger when one has small platinum and ceria NPs. The dissociation of water is frequently the rate-determining step for the WGS reaction on metal or metal/oxide surfaces.[6,16−18] In TPD experiments, we found that the Pt/CeO_x/TiO_2(110) surfaces were able to dissociate water *all the way* to yield molecular H_2. Figure 9 displays TPD spectra acquired after dosing water onto the catalyst with the highest activity in Figure 8 (θ_{Pt} = 0.2 ML, 11% of the titania covered by CeO_x). None of the features seen in Figure 9 was observed in control experiments when water was not dosed onto the Pt/CeO_x/TiO_2(110) surface. The strong H_2O peak near 180 K matches desorption temperatures found for water on TiO_2(110), CeO_2(111), and Pt(111).[35,36] The H_2O desorption features seen between 200 and 350 K were also observed after the molecule was dosed onto plain CeO_x/TiO_2(110). On the other hand, the H_2 desorption peak from 400 to 500 K and the O_2 desorption features between 550 and 700 K are *all unique* to the Pt/CeO_x/TiO_2(110) system and come from the full decomposition of water on the supported Pt NPs.

Our DFT calculations also point to facile dissociation of water on small Pt clusters electronically perturbed by interactions with ceria. We investigated the dissociation of water on Pt(111), on free Pt_{79} and Pt_8 particles,[25,26] and at Pt_8−ceria interfaces (see the corresponding structures in Figure 10). These systems were chosen taking into consideration previous studies showing that the activities of very small metal clusters supported on SiO_2 and MgO are very different from that of larger clusters.[37,38] The Pt_{79} and Pt_8 particles contain corner and edge atoms that have a coordination number significantly smaller that that of the atoms in a Pt(111)

dx.doi.org/10.1021/ja302070k | J. Am. Chem. Soc. 2012, 134, 8968−8974

surface.[25,26] Pt_8 is highly fluxional and undergoes geometrical changes upon bonding of water or after interaction with $CeO_2(111)$. The atoms of Pt_8 in contact with the $CeO_2(111)$ surface (Figure 10d) or with the $Ce_{40}O_{80}$ NP (Figure 10e) are strongly bound to the oxygen sites of the oxide support with a net Pt → ceria charge transfer.[25,26] The systems studied in Figure 10 allowed us to separate changes in reactivity due to variations in the coordination number of the Pt atoms [obtained by comparing the results for Pt(111) and Pt_{79} or Pt_8] from changes in reactivity caused by the interaction of Pt with the ceria support [obtained by comparing the results for free Pt_8 and Pt_8 in contact with $CeO_2(111)$ or the $Ce_{40}O_{80}$ NP].

Previous experimental[39] and theoretical studies[7,15] indicated that Pt(111) has problems adsorbing and dissociating the water molecule and is not a good WGS catalyst.[15] The dissociation of water on Pt(111) was calculated to be an endothermic process (Figure 11), in agreement with recent calorimetric measurements.[40] The calculated exothermicity of the $H_2O \rightarrow H + OH$ reaction increased in going from Pt(111) to the free Pt_{79} NP and even more in going to the free Pt_8 NP. The corner atoms present in the Pt_{79} and Pt_8 NPs (Figure 10) facilitate cleavage of the O−H bonds, and a small particle like Pt_8 is more fluxional than Pt_{79} in accommodating the reaction products (OH + H). These results indicate that the smaller the Pt particles, the easier the dissociation of water. This could explain the trends shown in Figures 2 and 8 for the variation of the WGS activity with Pt coverage. Furthermore, the DFT calculations showed an enhancement of the ability of Pt_8 to cleave O−H bonds when this cluster is deposited on a $CeO_2(111)$ surface or on a $Ce_{40}O_{80}$ NP. For example, the adsorption of H_2O on $Pt_8/CeO_2(111)$ leads to an energy release of ~1 eV that can be used to overcome the barrier for O−H bond cleavage. The resulting OH can react with CO, eventually yielding H_2 and CO_2 via the WGS reaction. The key to the chemical activity of $Pt_8/CeO_2(111)$ lies in the electronic perturbations induced by ceria on Pt_8. Thus, the ceria-supported Pt_8 appears as a fluxional system that can change geometry and charge distribution to allow better accommodation of adsorbates. Compared with other WGS catalysts such as $Cu/CeO_2(111)$ and $Au/CeO_2(111)$,[20] the $Pt/CeO_2(111)$ system has the unique property that the admetal is able to dissociate water in an efficient way. This is not the case for $Cu/CeO_2(111)$ or $Au/CeO_2(111)$, where water must dissociate on the oxide or at the oxide−metal interface.[20] Thus, small NPs of Pt in contact with CeO_2 can perform all the steps of the WGS reaction, making this system more active than Cu/CeO_2, Au/CeO_2, or Ni/CeO_2 (Figure 4). In addition, for $Pt/CeO_x/TiO_2$, the transfer of O from the ceria NPs to Pt (Figure 7 and ref 26) opens new paths that facilitate the dissociation of water on Pt ($O_{ads} + H_2O \rightarrow 2OH_{ads}$),[39] and one could also easily move O produced by the dissociation of water on ceria[23] to Pt for subsequent reaction with CO. A generally accepted mechanism for the WGS reaction does not yet exist.[5,6] Alternatives include associative mechanisms (i.e., formation of HCOO, HOCO, CO_3, or HCO_3 intermediates) and the redox mechanism.[6−17] In any case, none of the traditional mechanisms takes into consideration a transfer of oxygen from the oxide support (ceria) to the admetal (Pt) that can affect the formation and stability of intermediates and be an important factor in the extremely high WGS activity of $Pt/CeO_x/TiO_2$.

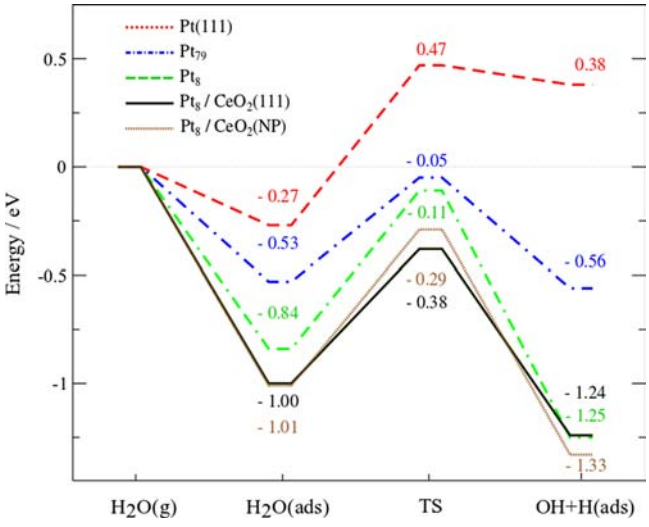

Figure 11. DFT-calculated energy profiles for the dissociation of water on Pt(111), Pt_{79} and Pt_8 clusters, and Pt_8 on $CeO_2(111)$ or a $Ce_{40}O_{80}$ NP. Figure 10 shows the calculated structures for the dissociation reaction.

In the literature of heterogeneous catalysis, it is well-known that the reactivity of the Pt/TiO_2 system can be affected by strong metal−support interactions.[3,41] These interactions usually deactivate platinum and involve the decoration of the surface of the Pt particles with small aggregates of titania after reduction in H_2 at very high temperature (>770 K).[41] This is completely different from the phenomena seen here, *where admetal ↔ oxide electronic interactions significantly enhance the catalytic activity of Pt*: $Pt(111) \ll Pt/CeO_2(111) < Pt/CeO_x/TiO_2(110)$. One must look for this type of interaction when designing metal/oxide catalysts that contain Pt. For example, we have found that the type of interaction that occurs on Pt/CeO_2 does not exist when Pt NPs are deposited on surfaces of alumina or silica. Thus, the Pt/Al_2O_3 and Pt/SiO_2 systems exhibit WGS activities that are 10−20 times smaller than that of Pt/CeO_2 and comparable to that of clean Pt(111).

SUMMARY AND CONCLUSIONS

The results of valence photoemission measurements and DFT calculations point to a new type of "strong metal−support interaction" for small Pt particles in contact with ceria. UPS spectra for the valence region of the $Pt/CeO_2(111)$ and $Pt/CeO_x/TiO_2(111)$ systems exhibited a density of Pt 5d states near the Fermi level that is much smaller than that expected for bulk metallic Pt. The Pt ↔ ceria interactions significantly enhance the ability of the admetal to adsorb water and dissociate the O−H bonds in the molecule. In going from Pt(111) to $Pt_8/CeO_2(111)$, the dissociation of water becomes a very exothermic process ($\Delta E = -1.3$ eV). Ceria-supported Pt_8 appears as a fluxional system that can change geometry and charge distribution to allow better accommodation of adsorbates such as H_2O, OH, and H. Compared with other WGS catalysts [Cu(111), Pt(111), $Cu/CeO_2(111)$, and $Au/CeO_2(111)$], the $Pt/CeO_2(111)$ surface has the unique property that the admetal is able to adsorb and dissociate water in an efficient way. XPS spectra taken after codeposition of Pt and CeO_x NPs on $TiO_2(110)$ point to a transfer of O from the ceria to Pt that opens new paths for the WGS process and makes the mixed-metal oxide an extremely active catalyst for the production of hydrogen. In TPD experiments, the Pt/

dx.doi.org/10.1021/ja302070k | J. Am. Chem. Soc. 2012, 134, 8968−8974

$CeO_x/TiO_2(110)$ surfaces were able to dissociate water fully into molecular H_2 and O_2.

AUTHOR INFORMATION

Corresponding Author

rodrigez@bnl.gov

Notes

The authors declare no competing financial interest.

ACKNOWLEDGMENTS

The work at BNL was financed by the U.S. Department of Energy (DOE), Office of Basic Energy Sciences, Chemical Sciences Division (DE-AC02-98CH10086). Calculations were carried out on the MARENOSTRUM supercomputer at the Barcelona Supercomputer Center. A.B. acknowledges the Spanish MICINN for a predoctoral grant. J.E. thanks INTEVEP and IDB for research grants that made possible part of this work at the Universidad Central de Venezuela.

REFERENCES

(1) Campbell, C. T. *Surf. Sci. Rep.* **1997**, *27*, 1−111.
(2) Farmer, J. A.; Campbell, C. T. *Science* **2010**, *329*, 933−936.
(3) (a) Tauster, S. J.; Fung, S. C.; Garten, R. L. *J. Am. Chem. Soc.* **1978**, *100*, 170−175. (b) Tauster, S. J. *Acc. Chem. Res.* **1987**, *20*, 389−394.
(4) (a) Diebold, U. *Surf. Sci. Rep.* **2003**, *48*, 53−229. (b) Pesty, F.; Steinrück, H.-P.; Madey, T. E. *Surf. Sci.* **1995**, *339*, 83−95.
(5) Hinrinchsen, K.-O.; Kochloefl, K.; Muhler, M. In *Handbook of Heterogeneous Catalysis*; Ertl, G., Knözinger, H., Schüth, F., Weitkamp, J., Eds.; Wiley-VCH: Weinheim, Germany, 2008.
(6) Burch, R. *Phys. Chem. Chem. Phys.* **2006**, *8*, 5483−5495.
(7) Zhai, Y.; Pierre, D.; Si, R.; Deng, W.; Ferrin, P.; Nilekar, A. U.; Peng, G.; Herron, J. A.; Bell, D. C.; Saltsburg, H.; Mavrikakis, M.; Flytzani-Stephanopoulos, M. *Science* **2010**, *329*, 1633−1636.
(8) Jacobs, G.; Williams, L.; Graham, U.; Thomas, G. A.; Sparks, D. E.; Davis, B. H. *Appl. Catal., A* **2003**, *252*, 107−118.
(9) Bunluesin, T.; Gorte, R. J.; Graham, G. W. *Appl. Catal., B* **1998**, *15*, 107−114.
(10) Phatak, A. A.; Koryabkina, N.; Rai, S.; Ratts, J. L.; Ruettlinger, W.; Farruto, R. J.; Blau, G. E.; Delgass, W. N.; Ribeiro, F. H. *Catal. Today* **2007**, *123*, 224−234.
(11) Lida, H.; Kondo, K.; Igarashi, A. *Catal. Commun.* **2006**, *7*, 240−244.
(12) Panagiotopoulou, P.; Christodoulakis, A.; Kondarides, D. I.; Boghosian, S. *J. Catal.* **2006**, *240*, 114−125.
(13) Kalamaras, C. M.; Gonzalez, I. D.; Navarro, R. M.; Fierro, J. L. G.; Efstathiou, A. M. *J. Phys. Chem. C* **2011**, *115*, 11595−11610.
(14) Gonzalez, I. D.; Navarro, R. M.; Wen, W.; Marinkovic, N.; Rodriguez, J. A.; Rosa, F.; Fierro, J. L. G. *Catal. Today* **2010**, *149*, 372−379.
(15) Flaherty, D. W.; Yu, W.-Y.; Pozun, Z. D.; Henkelman, G.; Mullins, C. B. *J. Catal.* **2011**, *282*, 278−288.
(16) Nakamura, J.; Campbell, J. M.; Campbell, C. T. *J. Chem. Soc., Faraday Trans.* **1990**, *86*, 2725−2730.
(17) Gokhale, A. A.; Dumesic, J. A.; Mavrikakis, M. *J. Am. Chem. Soc.* **2008**, *130*, 1402−1414.
(18) Rodriguez, J. A.; Graciani, J.; Evans, J.; Park, J. B.; Yang, F.; Stacchiola, D.; Senanayake, S. D.; Ma, S.; Perez, M.; Liu, P.; Sanz, J. F.; Hrbek, J. *Angew. Chem., Int. Ed.* **2009**, *48*, 8047−8050.
(19) Park, J. B.; Graciani, J.; Evans, J.; Stacchiola, D.; Ma, S.; Liu, P.; Nambu, A.; Sanz, J. F.; Hrbek, J.; Rodriguez, J. A. *Proc. Natl. Acad. Sci. U.S.A.* **2009**, *106*, 4975−4980.
(20) Rodriguez, J. A.; Liu, P.; Hrbek, J.; Evans, J.; Perez, M. *Angew. Chem., Int. Ed.* **2007**, *46*, 1329−1332.
(21) Mullins, D. R.; Radulovic, P. V.; Overbury, S. V. *Surf. Sci.* **1999**, *429*, 186−194.
(22) Lu, J. L.; Gao, H. J.; Shaikhutdinov, S. K.; Freund, H. J. *Catal. Lett.* **2007**, *114*, 8−16.
(23) Park, J. B.; Graciani, J.; Evans, J.; Stacchiola, D.; Senanayake, S. D.; Barrio, L.; Liu, P.; Sanz, J. F.; Hrbek, J.; Rodriguez, J. A. *J. Am. Chem. Soc.* **2010**, *132*, 356−363.
(24) Kresse, G.; Hafner, J. *Phys. Rev. B* **1993**, *47*, 558−561.
(25) Bruix, A.; Migani, A.; Vayssilov, G. N.; Neyman, K. M.; Libuda, J.; Illas, F. *Phys. Chem. Chem. Phys.* **2011**, *13*, 11384−11392.
(26) Vayssilov, G. N.; Lykhach, Y.; Migani, A.; Staud, T.; Petroval, G. P.; Tsud, N.; Skála, T.; Bruix, A.; Illas, F.; Prince, K. C.; Matolín, V.; Neyman, K. M.; Libuda, J. *Nat. Mater.* **2011**, *10*, 310−315.
(27) Migani, A.; Vayssilov, G. N.; Bromley, S. T.; Illas, F.; Neyman, K. M. *Chem. Commun.* **2010**, *46*, 5936−5938.
(28) Loschen, C.; Carrasco, J.; Neyman, K. M.; Illas, F. *Phys. Rev. B* **2007**, *75*, No. 035115.
(29) Zhou, Y.; Perket, J.; Zhou, J. *J. Phys. Chem. C* **2010**, *114*, 11853.
(30) (a) Paffett, M. T.; Gebhard, S. C.; Windham, R. G.; Koel, B. *J. Phys. Chem.* **1990**, *94*, 6831−6839. (b) Pirug, G.; Bonzel, H. P.; Broden, G. *Surf. Sci.* **1982**, *122*, 1−20.
(31) Senanayake, S. D.; Evans, J.; Agnoli, S.; Barrio, L.; Chen, T.-L.; Hrbek, J.; Rodriguez, J. A. *Top. Catal.* **2011**, *54*, 34−41.
(32) Park, J. B.; Conner, S. F.; Chen, D. A. *J. Phys. Chem. C* **2008**, *112*, 5490−5500.
(33) Larese, C.; Cabello Galisteo, F.; Lopez Granados, M.; Mariscal, R.; Fierro, J. L. G.; Lambrou, P. S.; Efstathiou, A. M. *J. Catal.* **2004**, *226*, 443−456.
(34) Parkinson, C. R.; Walker, M.; McConville, C. F. *Surf. Sci.* **2003**, *545*, 19−33.
(35) Zehr, R. T.; Henderson, M. A. *Surf. Sci.* **2008**, *602*, 1507−1516.
(36) Clay, C.; Haq, S.; Hodgson, A. *Phys. Rev. Lett.* **2004**, *92*, No. 046102.
(37) Vajda, S.; Winans, R. E.; Elam, J. W.; Lee, B.; Pellin, M. J.; Seifert, S.; Tikhonov, G. Y.; Tomczyk, N. A. *Top. Catal.* **2006**, *39*, 161−166.
(38) Heiz, U.; Sanchez, A.; Abbet, S.; Schneider, W.-D. *Chem. Phys.* **2000**, *262*, 189−200.
(39) (a) Fischer, G. B.; Sexton, B. A. *Phys. Rev. Lett.* **1980**, *44*, 683−686. (b) Bedürftig, K.; Volkening, S.; Wang, Y.; Wintterlin, J.; Jacobi, K.; Ertl, G. *J. Chem. Phys.* **1999**, *111*, 11147−11154.
(40) Lew, W.; Crowe, M. C.; Karp, E.; Lytken, O.; Farmer, J. A.; Arnadottir, L.; Schoenbaum, C.; Campbell, C. T. *J. Phys. Chem. C.* **2011**, *115*, 11586−11594.
(41) Datye, A. K.; Kalakkad, D. S.; Yao, M. H.; Smith, D. J. *J. Catal.* **1995**, *155*, 148−153.